Ionic Silver Amino Complexes Displaying Liquid Crystalline Behavior Close to Room Temperature

Ana C. Albéniz,[a] Joaquín Barberá,[b] Pablo Espinet*,[a] M. Carmen Lequerica,[a] Anne M. Levelut,[c] F. Javier López-Marcos,[b] and José L. Serrano*[a]

Keywords: Metallomesogens / Liquid crystals / Silver / N ligands / Amines

The liquid crystalline properties of a series of ionic silver complexes $[Ag(NH_2n\text{-}C_nH_{2n+1})_2]X$ (X = NO_3, n = 6, 8, 10, 12, 14; X = BF_4, n = 8, 10, 12, 14), derived from silver nitrate or tetrafluoroborate and aliphatic amines, have been investigated by optical microscopy, DSC, and X-ray diffraction. The materials exhibit a birefringent fluid phase identified as a smectic A mesophase by optical microscopy and X-ray diffraction. Some of the complexes are liquid crystalline at temperatures close to room temperature. The X-ray results are consistent with the existence in the mesophase of a bilayer organization. The silver cations adopt a U-shape, which allows for the adoption of this bilayer arrangement, with alternating ionic and apolar regions and a short-range square-planar array inside the cationic sublayers. The thermodynamic parameters suggest that the melting transition clearly involves only disorder (melting) of the chains, whereas the clearing transition implies breaking the anion-cation arrangement.

Introduction

Metallomesogens (metal complexes that are formed with organic ligands and exhibit liquid crystalline behavior) have considerably enhanced the field of liquid crystals.[1] The vast majority of metallomesogens reported so far have a rod- or disk-shaped rigid core (usually with aryl rings) bearing long hydrocarbon tails. Ionic amphiphilic metal complexes have been reported less frequently.[2]

In this paper we report the synthesis and liquid crystalline properties of two series of ionic silver complexes, both of which are based on apparently simple coordination compounds $[Ag(NH_2n\text{-}C_nH_{2n+1})_2]X$ (X = NO_3, n = 6, 8, 10, 12, 14; X = BF_4, n = 8, 10, 12, 14). These compounds appear to be deceptively simple as they are similar in stoichiometry and metal coordination to other compounds based on 4-substituted pyridines {$[AgL_2]X$; L = 4-substituted pyridine; X = alkyl sulfate, BF_4, CF_3SO_3, NO_3, PF_6}.[3] In fact they turn out to be structurally very different: the cation, which lacks rigid rings, has a flexible aliphatic structure that is able to adopt any shape, whereas in the pyridine derivatives previously reported, the cation has, by necessity, an extended central rigid rod-like geometry. In this respect the complexes reported here are more similar to the U-shaped structures found for *trans*-$[PdCl_2\{PEt_2(O\text{-}chl)\}_2]$ (chl = cholesteryl)[4] and for the silver complexes [AgL]X with the macrocyclic ligand 1,10-bis[4-(dodecyloxy)-benzoyl]-1,10-diaza-4,7,13,16-tetrathiacyclooctadecane.[5] Thus the complexes reported in this paper combine a number of unusual features: (i) their mesogenic behavior appears at rather low temperatures; (ii) the metal is included in the promesogenic cation; (iii) X-ray characterization of their mesophases supports a bilayer structure reminiscent of that observed in classical lyotropic bilayer mesophases, with the cation adopting a U-shaped geometry comparable to that observed in phospholipid-based lyotropic derivatives.

[a] Departamento de Química Inorgánica, Facultad de Ciencias, Universidad de Valladolid,
E-47005 Valladolid, Spain
E-mail: espinet@qi.uva.es
[b] Química Orgánica, Facultad de Ciencias-ICMA, Universidad de Zaragoza-CSIC,
E-50009 Zaragoza, Spain
[c] Laboratoire de Physique des Solides, Bâtiment 510, Université Paris-Sud,
F-91405 Orsay Cédex, France

Results and Discussion

Synthesis

The complexes were prepared by the stoichiometric reaction of the appropriate silver salt, AgX, and the corresponding alkylamine in acetonitrile (Equation 1), and were isolated as crystalline solids. They are light-sensitive and their preparation and handling must be carried out in the dark. However, they can survive moderately long exposure to light, such as the periods required for the microscopy studies.

$$AgX + 2\ NH_2n\text{-}C_nH_{2n+1} \rightarrow [Ag(NH_2n\text{-}C_nH_{2n+1})_2] \quad (1)$$

Microscopy Studies

Optical microscopy with polarized light revealed that the solids melt, upon heating, to a fluid phase exhibiting a dark homeotropic texture with some elongated bright birefringent regions. At a higher temperature the texture disappears, with the fluid phase becoming isotropic. Upon cooling the resultant isotropic liquid, some *bâtonnets* are formed at the transition point to the mesophase, but they immediately disappear to leave a homeotropic texture consisting of dark areas scattered, in some cases, with small

  1434−1948/00/0101−0133 $ 17.50+.50/0

focal-conic domains and Maltese crosses. This behavior is typical of a fluid lamellar (S_A) mesophase.[6] All the compounds studied underwent some decomposition when exposed to air and visible light in the isotropic state. Therefore extended heating and repeated heating-cooling cycles are to be avoided.

DSC Studies

The DSC data are collected in Table 1. The thermograms show two endothermic peaks on heating (exothermic on cooling) corresponding to the solid-to-mesophase and the mesophase-to-liquid transitions. Occasionally, small endothermic peaks were observed in the first heating scan at temperatures below the melting point (crystal-crystal transitions or pre-melting phenomena) but these were not usually observed in subsequent cooling or reheating scans. The existence of the liquid crystal phase at very low temperatures (compared to common metallomesogens) for the short chain derivatives is noteworthy. The mesophases of some complexes can be supercooled to below room temperature.

In the two series of complexes (nitrates and tetrafluoroborates) the melting temperatures increase steadily with the number of carbon atoms in the hydrocarbon chains (Table 1). The clearing temperatures increase with the number of carbon atoms for short chains, reach a maximum, and decrease for the longer chains. In each series the melting molar enthalpy $(\Delta H_M)_{melt}$ and entropy $(\Delta S_M)_{melt}$ values increase steadily with the number of carbon atoms in the aliphatic amine (Table 1), and are very different from one series (NO_3^-) to the other (BF_4^-). In contrast, the clearing molar enthalpy and entropy values, $(\Delta H_M)_{clear}$ and $(\Delta S_M)_{clear}$, decrease steadily upon increasing the number of carbon atoms in the aliphatic chain. A closer examination can be made by means of a crude but informative linear plot of these values against number of carbon atoms in the chain.

Table 1. Optical, thermal and thermodynamic data of $[Ag(NH_2\text{-}C_nH_{2n+1})_2]X$ complexes (C: crystal; S_A: smectic A mesophase; I: isotropic liquid).

X	*n*	Transition	T [°C]	ΔH [kJ·mol^{-1}]	ΔS [J·K^{-1}·mol^{-1}]
NO_3	6	C−S_A	37.8	14.6	47.0
		S_A−I	118.2	4.3	11.0
NO_3	8	C−S_A	54.8	19.9	60.7
		S_A−I	141.3	4.0	9.7
NO_3	10	C−S_A	67.0	25.2	74.1
		S_A−I	141.3	3.3	8.0
NO_3	12	C−S_A	76.7	31.7	90.6
		S_A−I	138.6	2.7	6.6
NO_3	14	C−S_A	79.7	36.6	103.7
		S_A−I	131.9	2.3	5.7
BF_4	8	C−S_A	39.5	38.3	122.5
		S_A−I	113.5	3.8	9.8
BF_4	10	C−S_A	53.4	49.1	150.4
		S_A−I	129.8	3.5	8.7
BF_4	12	C−S_A	59.9	62.1	186.5
		S_A−I	137.4	2.8	6.8
BF_4	14	C−S_A	67.0	68.2	200.5
		S_A−I	131.7	2.5	6.2

The fitting of the lines for $(\Delta H_M)_{melt}$ is remarkably good for both series (Figure 1). The slope affords the contribution to the melting enthalpy per carbon atom in the cation and the values are $(\Delta H_C)_{melt}$ = 1.395 kJ·mol^{-1} for the NO_3^- series and 2.568 kJ·mol^{-1} for the BF_4^- series. The fit for $(\Delta S_M)_{melt}$ is also quite good and affords values of $(\Delta S_C)_{melt}$ = 3.583 J·K^{-1}·mol^{-1} for the NO_3^- series and 6.753 J·K^{-1}·mol^{-1} for the BF_4^- series. The $(\Delta H_M)_{melt}$ and $(\Delta S_M)_{melt}$ values extrapolated for $n = 0$ (even though they lack a rigorous physical meaning are in all cases very small compared to the value $2n(\Delta H_C)_{melt}$ or $2n(\Delta S_C)_{melt}$, even for the shortest chains. This indicates that the melting enthalpy and melting entropy values almost exclusively arise due to the chains and, hence, the melting transition mainly involves melting of the chains, whereas the anion-cation interactions seem to be hardly affected. The nature of the anion, however, clearly affects the ΔH_C and ΔS_C values, which are almost twice as high for the BF_4^- series than for the NO_3^- series. In a purely ionic anion-cation interaction no difference should be expected, thus this effect is a reflection of some covalent donor interaction from the anion to the silver center. Such an interaction would be expected to be higher from the O atoms of the NO_3^- than from the F atoms of the BF_4^-.[7] Consequently, the silver atom becomes less of an acceptor towards the amine when the anion is NO_3^-, the chain is less polarized, and the chain interactions diminish, as is observed.

The fitting of the lines for $(\Delta H_M)_{clear}$ and $(\Delta S_M)_{clear}$ is also acceptable for both series (Figure 2). The slopes in this case are small and negative. The intercepts at $n = 0$ are comparatively high and are similar for both anions: about 5.9 kJ·mol^{-1} for $(\Delta H_M)_{clear}$ and 15.0 J·K^{-1}mol^{-1} for $(\Delta S_M)_{clear}$. This suggests that the clearing transition is mainly due to the melting of the anion-cation arrangement. The actual values are tuned by the size of the cation, with the transition becoming easier for the bulkier the cation.

X-ray Studies

X-ray diffraction experiments were carried out on magnetically oriented mesophases of three nitrate complexes (hexylamine, octylamine, and decylamine derivatives) and one tetrafluoroborate complex (octylamine derivative).

Two regions can be distinguished in the X-ray patterns {Figure 3 shows the pattern of $[Ag(octylamine)_2]BF_4$ at 50 °C}. In the low angle region a set of sharp arcs (labelled A), which extend over ±20° around the magnetic field direction, correspond to lattice spacing ratios 1, 1/2, 1/3, etc., and are characteristic of a lamellar system. The layer periodicity *d* is 18.8 Å, 22.5 Å, and 27.0 Å for the hexylamine, octylamine, and decylamine nitrate complexes, respectively, and 21.9 Å for the octylamine tetrafluoroborate complex (Table 2). In the wide-angle region the long-exposure time patterns exhibit two diffuse rings, both showing a large azimuthal spreading. The intensity maxima correspond to mean distances $l/(2\sin\theta) = 2\pi\cdot q^{-1}$ that are equivalent to 6.3−6.4 Å (labelled B) and 4.5 Å (labelled C).

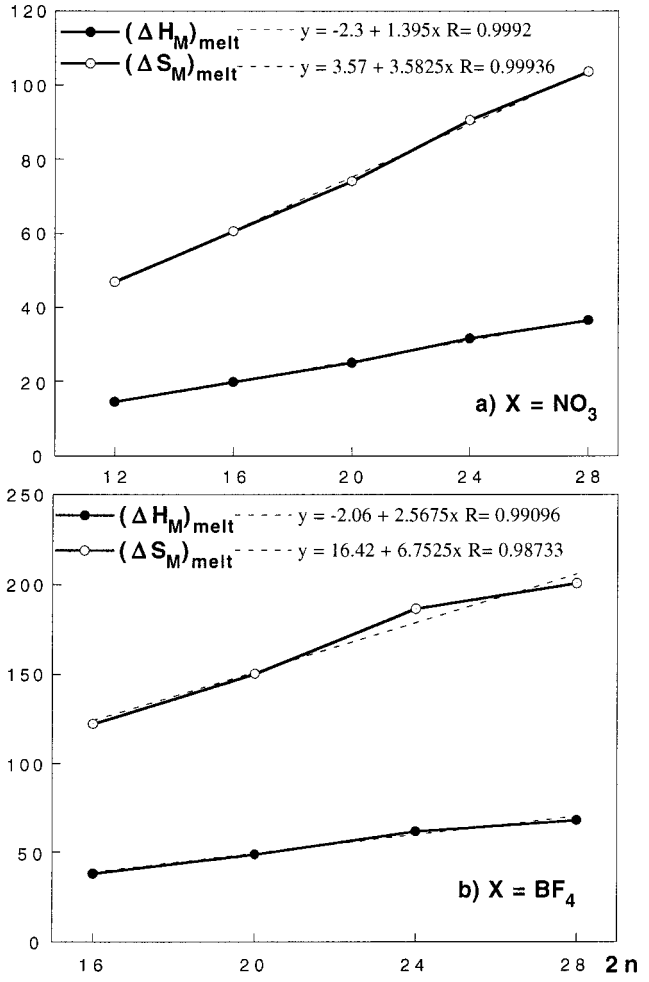

Figure 1. Plot of melting molar enthalpy $(\Delta H_M)_{melt}$ and entropy $(\Delta S_M)_{melt}$ values versus the total number of carbon atoms in the complex, $2n$, for: (a) $[Ag(NH_2n\text{-}C_nH_{2n+1})_2]NO_3$; (b) $[Ag(NH_2n\text{-}C_nH_{2n+1})_2]BF_4$.

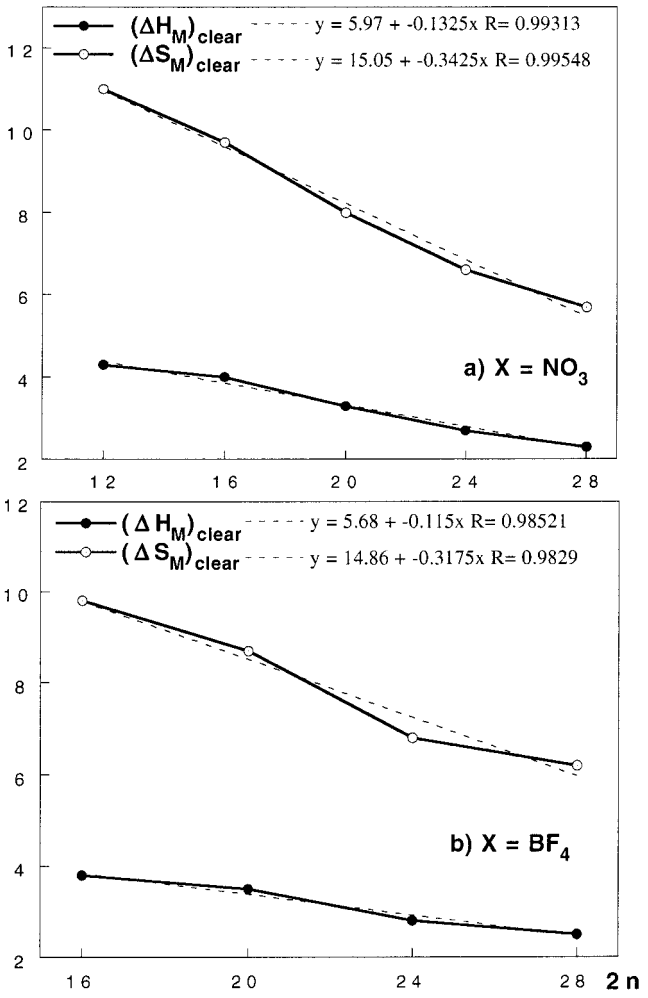

Figure 2. Plot of clearing molar enthalpy $(\Delta H_M)_{clear}$ and entropy $(\Delta S_M)_{clear}$ values versus the total number of carbon atoms in the complex, $2n$, for: (a) $[Ag(NH_2n\text{-}C_nH_{2n+1})_2]NO_3$; (b) $[Ag(NH_2n\text{-}C_nH_{2n+1})_2]BF_4$.

The only set of sharp reflections observed corresponds to the lamellar structure and therefore there is no periodic intra-lamellar order. Moreover, this set of arcs is aligned along the magnetic field and confirms the existence of a smectic A mesophase. The number of observed reflections on the layer planes is higher than usual for thermotropic smectic phases, although the intensities of these reflections decrease monotonically as the scattering vector is increased. Therefore the heavy components of the complex, namely the silver atom and the anion, are located in a thin slab of the smectic layer. Moreover, it is possible to give an estimation of the positional fluctuations of the heavy components of the layer from the Debye−Waller factor, $\exp(-2q\langle u^2\rangle)$. If this factor is equal to 10^{-6} for the fourth order ($q = 4 \times 2\pi/d$), the average extension of the heavy sublayer will be equal to a tenth of the total layer thickness d.

The diffuse ring at 4.5 Å is characteristic of a molten paraffinic medium. The mosaic spread of the smectic planes is large and consequently it is not possible to determine the degree of orientational order of the chains. However, since

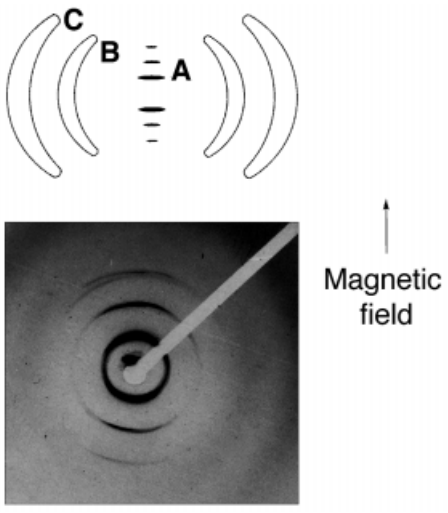

Figure 3. X-ray diffraction pattern of the magnetically aligned mesophase of $[Ag(NH_2n\text{-}C_8H_{17})_2]BF_4$ (at 50°C) along with a schematic interpretation of the pattern.

Table 2. Distances [Å] in $[Ag(NH_2n\text{-}C_nH_{2n+1})_2]X$ complexes measured in the mesophase by X-ray diffraction

X	n	d_A	d_B	d_C
NO_3	6	18.8	6.3	4.5
NO_3	8	22.5	–	–
NO_3	10	27.0	–	–
BF_4	8	21.9	6.4	4.5

the ring is nearly isotropic, the chains are likely to be poorly oriented. The second diffuse ring at 6.4 Å reveals that the intralayer ordering is more complex than for usual rod-like smectogenic molecules. The fact that 6.4 Å $\sqrt{4.5} \approx 2$ Å is consistent with a short range square array. However, it is important to note that, given the intensity of the diffuse ring at 4.5 Å, it cannot be simply considered as a second order maximum arising from a local square primitive cell with a lattice constant of 6.4 Å. It rather suggests that the equatorial scattering pattern results from the superposition of two different lattices, the area of one (approximately 6.4 Å × 6.4 Å = 41 Å^2) being twice as much as the area of the other (approximately 4.5 Å × 4.5 Å = 20 Å^2). It is important to note that an area of 41 Å^2 corresponds to twice the cross-sectional area of a hydrocarbon chain in an quasiextended conformation.[8]

The results described above, as well as density criteria, are consistent with the presence of two $[AgL_2]X$ units in the tetragonal cell that are arranged in such a way that the chain-to-chain distance is about 4.5 Å and the mean distance of 6.4 Å describes the ordering of the polar head groups. All these requirements can only be fulfilled if the silverdiamine cations adopt a U-shape and arrange themselves in a bilayer structure (Figure 4). The silver atoms form a square-planar local array of 6.4 Å size, and the aliphatic chains extend on each side of a central slab containing the polar groups in such a way that the two hydrocarbon chains belonging to the same cation point in the same direction. This arrangement is adequate to fill space efficiently and accommodate the anions between these layers, where a good anion-cation electrostatic interaction (with some covalent component for the nitrate series, as discussed above) can be obtained. Figure 5 and Figure 6 show a space-filling model of this kind of arrangement. Clearly the intralayer order in the mesophase must be lower and also just local. This structure is comparable to the L_δ phase observed in phospholipid-based lyotropic systems.[6] A bilayer organization of U-shaped cations has also been found in some thermotropic ionic metallomesogens based on macrocyclic N,S-containing ligands.[5] However, in that case the in-plane order does not correspond to a local square lattice but to a periodic undulation of the ionic sublayer.

It is important to note that the scattering factors of a silver atom (47) and the anions (31 for NO_3^-, or 40 for BF_4^-) are quite similar. Consequently, these two components must be close to each other, both in the plane perpendicular to the director and in the direction parallel to the director, in order to make a contribution to the intensity scattered in the Bragg reflections and in the 6.4 Å and 4.5 Å rings. Assuming that the silver atoms in the proposed arrangement lie at the corners of the two-dimensional square lattice and the anions lie at the center of the square, the 4.5 Å ring would arise from chain-chain and cation-anion interferences, and the 6.4 Å ring from cation-cation and anion-anion interferences.

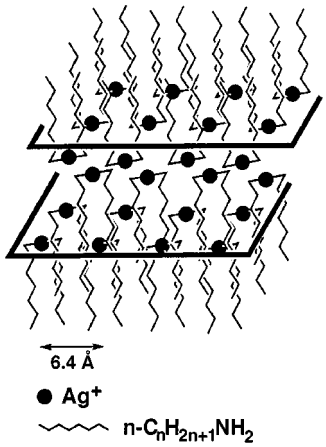

Figure 4. Model of a bilayer in the liquid crystal phase of $[Ag(NH_2n\text{-}C_nH_{2n+1})_2]X$ complexes (anions omitted).

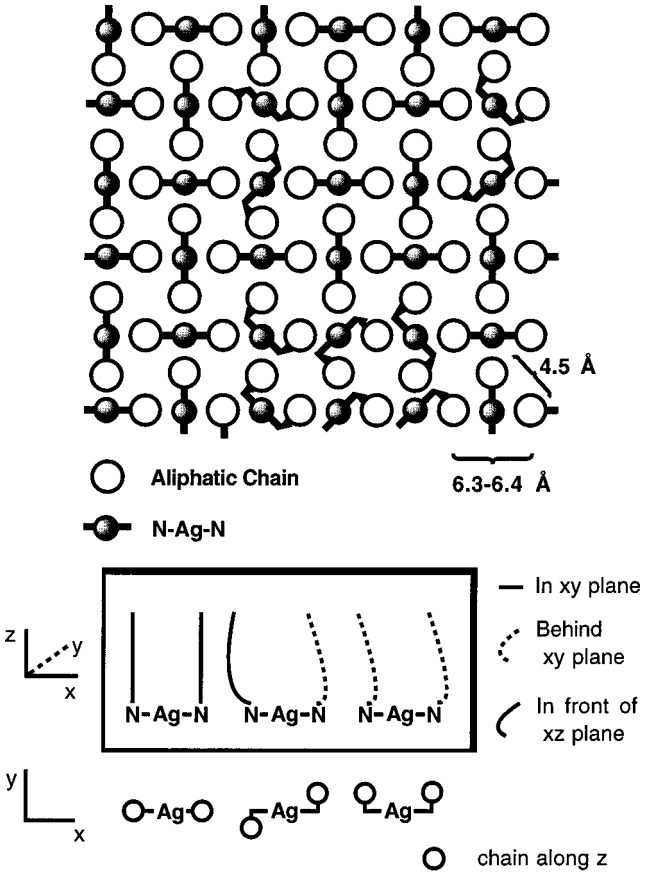

Figure 5. Sketch of the arrangement of the cations in the mesophase viewed along the director (perpendicular to the layer plane). The flexibility of the aliphatic chains allows different arrangements with respect to the N–Ag–N bond, which are a source of disorder and are illustrated in the lower part of the figure.

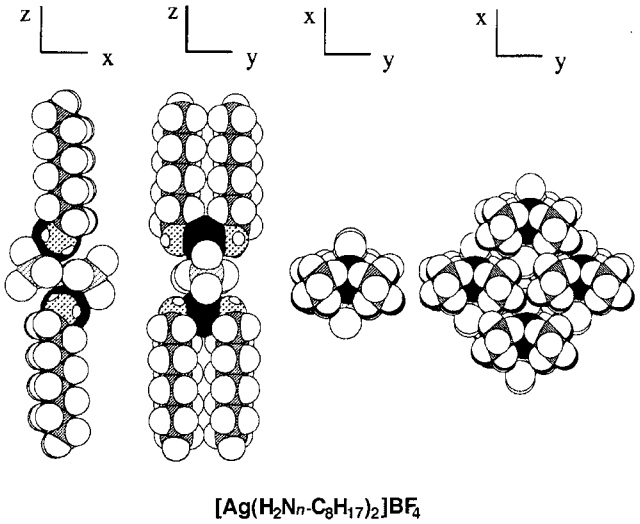

Figure 6. Space-filling model proposed for the complexes (X = BF_4). Left: possible arrangement of two anions and two cations (as the building block of the bilayers) viewed along the three axis. Right: packing of eight anions and eight cations (four up and four down) viewed along the z axis. Note that the overall packing results in a cylindrical cluster that should be able to rotate quite freely, thus introducing additional disorder. (Ag = black solid; N = large dots; B = small dots; C = shadow, H and F = white).

An alternative structural model could be proposed in which the local tetragonal unit cell contains one $[AgL_2]X$ unit per local cell. In this model the silverdiamine cation would sit at the four corners of the cell in an extended (rod-like) conformation parallel to the four-fold axis and the anions would be at the center of the cell. In this model the 4.5 Å ring would arise from anion-cation interferences and the 6.4 Å ring from anion-anion and cation-cation interferences. However, a tetragonal cell of width 6.4 Å and length *d* (Table 2) containing only one $[AgL_2]X$ unit would lead to very inefficient packing. Indeed, the density associated with this model would be too low (approximately 0.8 g cm^{-3}), and the average area per chain would be too large (S = 6.4 Å × 6.4 Å = 41 $Å^2$). Moreover, the intensity ratio of the two diffuse rings should be the reverse of that actually observed. Therefore this array, based on extended (rod-like) silverdiamine cations, is not consistent with the X-ray data and must be discounted. A similar structure with interdigitated layers would be consistent with the observed local order, but should lead to a layer thickness twice as small as that experimentally measured.

The bilayer model contains two molecules per unit cell, leading to a reasonable estimated density (approximately 1.6 g cm^{-3}), and fits all the X-ray data. The surface available for each paraffinic chain is about 20.0−20.5 $Å^2$ (S = 6.4 Å × 6.4 Å/2). Unfortunately we have not been able to grow single crystals of the complexes, but further support for the bilayer model comes from powder X-ray experiments carried out at room temperature on the decylamine nitrate complex. The powder pattern corresponds to a three-dimensional triclinic phase with parameters a = 5.03 Å, b = 8.84 Å, c = 27.2 Å, α = 93.0°, β = 93.3°, γ = 92.3°, with two molecules per unit cell. Parameter c is almost identical to the interlayer spacing (27.0 Å) found for the mesophase of the same compound (see Table 2). The fact that in the crystalline structure there are two molecules in a pseudo-rectangular section of approximately 5.0 Å × 8.8 Å = 44 $Å^2$ proves that is it possible for two molecules to be located in the two-dimensional square lattice of 41 $Å^2$ proposed for the mesophase. The calculated density of the crystal packing is 1.33 g cm^{-3}, whereas the density estimated for the mesophase is about 1.6 g cm^{-3}. This high value can be explained because it has been calculated on the basis of the diffraction data from the locally ordered areas in the mesophase. In fact, the square array has a short correlation range, and the presence of some rod-shaped molecules in with the U-shaped molecules cannot be ruled out. In addition, the orientational order of the chains is weak and the angle between the two chains of a molecule is widely fluctuating.

Finally, it is interesting to note that there are indications that the silverdiamine cations with long aliphatic primary amines may also adopt a U-shape in aqueous solution. In fact it has been reported that the values of ΔH^0 and ΔS^0 for the coordination of *n*-butyl- and *n*-pentylamine to Ag^+ are anomalous when compared with the values for the corresponding protonation reactions. It has been suggested that "a possible explanation for these anomalies is that there may be some hydrophobic interaction between the two ends of the hydrophobic chains". Clearly, although not explicitly stated, this implies the adoption of a U-shape.[9]

Conclusions

In summary, these simple silver coordination compounds reveal that metal cations can induce thermotropic behavior in non-mesogenic ligands, even if these ligands lack rigid cores and have only short aliphatic chains. Moreover, very low transition temperatures are obtained. The diffraction data support a bilayer model based on the packing of U-shaped silverdiamine cations. The thermodynamic parameters suggest that the melting transition involves only disorder (melting) of the chains, whereas the clearing transition involves breaking the anion-cation arrangement

Experimental Section

General: All compounds were satisfactorily characterized by IR spectroscopy and elemental microanalysis. − IR spectra were recorded on a Perkin−Elmer 1600 (series FTIR) spectrometer. − Microanalyses were performed with a Perkin−Elmer 240 B microanalyzer. − The optical textures of the mesophases were studied with a Meiji polarizing microscope equipped with a Mettler FP8 hot stage and an FP80 central processor. − The transition temperatures and enthalpies were measured by differential scanning calorimetry with a Perkin−Elmer DSC-7 instrument operated at a scanning rate of 10°C/min on heating. The apparatus was calibrated with indium (156.6°C; 28.4 $J \cdot g^{-1}$) as a standard. − X-ray diffraction experiments were carried out on magnetically aligned samples held in Lindemann glass capillary tubes of 1 mm diameter. The capillary tube, containing the sample, was set in an oven placed

between the poles of a magnet (magnetic field 0.3 T). The sample was irradiated with a point-focused X-ray beam (Cu-K_α radiation, $\lambda = 1.541$ Å) perpendicular to the magnetic field. The camera was evacuated in order to suppress air scattering. The diffraction patterns were collected on a flat film perpendicular to the X-ray beam. Powder experiments were carried out in a Guinier diffractometer (Huber 644) operating with a Cu-$K(\alpha_1)$ beam ($\lambda = 1.5405$ Å) issued from a germanium monochromator. The samples were held in rotating Lindemann glass capillaries (0.5 mm diameter) and the diffraction patterns were registered with a scintillation counter.

Preparation of $[Ag(NH_2n\text{-}C_nH_{2n+1})_2]NO_3$ ($n = 6$ and 8): A solution of $AgNO_3$ (0.255 g, 1.5 mmol) and amine (3.0 mmol) in acetonitrile (ca. 10 mL) was stirred at room temperature for 2 h. The resulting solution was concentrated under vacuum until crystallization began. Diethyl ether was added and the suspension was cooled in the freezer overnight. The white needles obtained were collected by filtration, washed with ether and dried under vacuum. Yield: 65% ($n = 6$) and 75% ($n = 8$). − Analytical data: ***n* = 6**: calcd. C 38.72, H 8.12, N 11.29); found C 38.31, H 8.25, N 11.30. −***n* = 8**: calcd. C 44.86, H 8.94, N 9.81; found C 44.74, H 9.31, N 9.79.

Preparation of $[Ag(NH_2n\text{-}C_nH_{2n+1})_2]NO_3$ ($n = 10$, 12 and 14): A suspension of $AgNO_3$ (0.221 g, 1.3 mmol) and amine (2.6 mmol) in acetonitrile (ca. 15 mL) was stirred at room temperature for 6 h. The resulting white suspension was concentrated under vacuum. Diethyl ether was added and the suspension was cooled in the freezer overnight. The crystallized product was collected by filtration, washed with ether and dried under vacuum. Yield: 70−90%. If necessary, the products can be further purified by recrystallization from acetonitrile/diethyl ether. − Analytical data ***n* = 10:** calcd. C 49.58, H 9.57, N 8.67; found C 49.79, H 10.04, N 8.63. − ***n* = 12:** calcd. C 53.32, H 10.07, N 7.77; found C 53.23, H 10.36, N 7.80. − ***n* = 14**: calcd. C 56.36, H 10.47, N 7.04; found C 56.51, H 10.50, N 6.93.

Preparation of $[Ag(NH_2n\text{-}C_nH_{2n+1})_2]BF_4$: A suspension of $AgBF_4$ (0.234 g, 1.2 mmol) and amine (2.4 mmol) in acetonitrile (ca. 10 mL) was stirred at room temperature under nitrogen for 6 h. The resulting solution ($n = 8$) or white suspension ($n = 10$, 12, 14) was concentrated under vacuum and cooled in the freezer overnight. The crystallized white product was collected by filtration, washed with ether and dried under vacuum. Yield: 60−75%. If necessary, the products can be further purified by recrystallization from acetonitrile/diethyl ether. − Analytical data ***n* = 8:** calcd. C 42.41, H 8.45, N 6.18; found C 42.61, H 8.83, N 6.30. − ***n* = 10:** calcd. C 47.17, H 9.10, N 5.50; found C 47.27, H 9.30, N 5.54. − ***n* = 12**: calcd. C 50.99, H 9.63, N 4.95; found C 51.40, H 10.01, N 4.91. − ***n* = 14**: calcd. C 54.11, H 10.06, N 4.51; found C 54.35, H 10.20, N 4.37.

Acknowledgments

This work was financed by the Comisión Interministerial de Ciencia y Tecnología (Spain, Projects MAT96-0708 and MAT97-0968-C02) and the Junta de Castilla y León (Project VA23/97).

[1] Reviews: A. M. Giroud-Godquin, P. M. Maitlis, *Angew. Chem.* **1991**, *103*, 370; *Angew. Chem. Int. Ed. Engl.* **1991**, *30*, 375; P. Espinet, M. A. Esteruelas, L. A. Oro, J. L. Serrano, E. Sola, *Coord. Chem. Rev.* **1992**, *117*, 215; D.W. Bruce in *Inorganic Materials* (Eds.: D. Bruce, D. O′Hare), Wiley, Chichester, **1992**, chapter 8; S. A. Hudson, P. M. Maitlis, *Chem. Rev.* **1993**, *93*, 861; *Metallomesogens. Synthesis, Properties and Applications* (Ed.: J. L. Serrano), VCH, Weinheim, **1996**; A. M. Giroud-Godquin in *Handbook of Liquid Crystals* (Eds.: D. Demus, J. Goodby, G. W. Gray, H.W. Spiess, D. V. Vill), Wiley-VCH, Weinheim, **1988**, Vol 2B, chapter 14.

[2] For a review of ionic metallomesogens see: F. Neve, *Adv. Mater.* **1996**, *8*, 277.

[3] D. W. Bruce, D. A. Dunmur, E. Lalinde, P. M. Maitlis, P. Styring, *Nature (London)* **1986**, 323, 791; D. W. Bruce, D. A. Dunmur, P. M. Maitlis, P. Styring, M. A. Esteruelas, L. A. Oro, M. B. Ros, J. L. Serrano, E. Sola, *Chem. Mater.* **1989**, *1*, 479; M. Marcos, M. B. Ros, J. L. Serrano, M. A. Esteruelas, E. Sola, L. A. Oro, J. Barberá, *Chem. Mater.* **1990**, *2*, 748; D. W. Bruce, D. A. Dunmur, S. A. Hudson, E. Lalinde, P. M. Maitlis, M. P. McDonald, R. Orr, P. Styring, A. S. Cherodian, R. M. Richardson, J. L. Feijoo, G. Ungar, *Mol. Cryst. Liq. Cryst.* **1991**, *206*, 79; H. Adams, N. A. Bailey, D. W. Bruce, S. C. Davis, D. A. Dunmur, P. D. Hempstead, S. A. Hudson, S. Thorpe, *J. Mater. Chem.* **1992**, *2*, 395; D. W. Bruce, S. A. Hudson, *J. Mater. Chem.* **1994**, *4*, 479; D. W. Bruce, B. Donnio, S. A. Hudson, A. M. Levelut, S. Megtert, D. Petermann, M. Veber, *J. Phys. II France* **1995**, *5*, 289; D. W. Bruce, S. Estdale, D. Guillon, B. Heinrich, *Liq. Cryst.* **1995**, *19*, 301.

[4] P. Verdagué, J. Courtieu, H. Adams, N. A. Bailey, P. M. Maitlis, *J. Chem. Soc., Chem. Commun.* **1994**, 1589.

[5] F. Neve, M. Ghedini, G. De Munno, A. M. Levelut, *Chem. Mater.* **1995**, *7*, 688.

[6] V. Luzzati in *Biological Membranes* (Ed.: D. Chapman), Academic Press, London, **1968**, Chap. 3; J. Charvolin, A. Tardieu in *Solid State Physics, Supplement 14* (Ed.: L. Liébert), Academic Press, New York, **1978**, pp. 209−257.

[7] Covalent interactions are found, for instance, in the X-ray structure of the pyrazine complex $[Ag(N_2C_4H_8)]_n(NO_3)_n$: R. G. Vranka, E. Lamma, *Inorg. Chem.* **1966**, *5*, 1020.

[8] A. A. Schaerer, C. J. Busso, A. E. Smith, L. B. Skinner, *J. Am. Chem. Soc.* **1955**, *77*, 2017.

[9] L. D. Hansen, D. J. Temer, *Inorg.Chem.* **1971**, *10*, 1439.

Received June 14, 1999
[I99218]